Thermal, mechanical, and electronic properties of glycine-sodium nitrate crystal

J. Hernández-Paredes, Daniel Glossman-Mitnik, O. Hernández-Negrete, H. Esparza-Ponce, M.E. Alvarez R, R. Rodríguez Mijangos, A. Duarte-Moller

Abstract

Glycine-sodium nitrate, $C_2H_5N_2NaO_5$ (GSN), crystals were grown from aqueous solutions by slow cooling with a temperature lowering rate of 1 °C/day in the range of 40–22 °C. These crystals were analyzed by differential thermal and thermogravimetric analysis (DTA-TGA) and mechanical hardness tester in order to obtain their thermal and mechanical properties. Mechanical characterization was done by studying the variation of microhardness with applied load. The dielectric properties of GSN were calculated by using the CASTEP code within the framework of the generalized gradient approximation (GGA). For better understanding of the optical properties of GSN, the second derivative of $\varepsilon_2(E)$ was evaluated. DTA-TGA analysis showed that the material has a thermal stability up to 198 °C. The microhardness test was carried out for several faces of GSN crystals, and the tests revealed a load dependence to hardness. Analysis of the second derivative of $\varepsilon_2(E)$ allowed to obtain better resolution of the electronic transitions involving the energy bands. Besides, a theoretical representation of the orbitals' energy diagram was obtained. A discussion about the relation of structure-properties and molecular character of GSN is presented here.

Introduction

The non-linear optics (NLO) field demands the development of new materials that have strong interaction with a light beam. Semi-organic compounds based on

aminoacids mixed with inorganic complexes have been found useful for second harmonic generation (SHG), process [1–4]. The purpose is to achieve the construction of useful devices such as: frequency doublers, active optical interconnects, and switches. These devices have great applications in telecommunications and signal processing [5].

However, it is known that, due to their molecular character and the large interatomic distances some of these compounds have poor thermal and mechanical properties. Unfortunately, such materials can be unstable at high temperatures. Moreover, due to their poor mechanical properties they are not adequate for processing. For these reasons, it is very important to analyze the thermal and mechanical properties of the new materials in order to recognize them as candidates for the fabrication of optical devices and photonic applications.

Computational chemistry using the density functional theory (DFT) for prediction of physical and chemical properties of new materials is widely employed nowadays. This tool offers the capability to study novel materials with a simple and inexpensive scheme, because it has proved to be effective predicting the properties of new materials with good agreement [6–8].

In our previous work [9], $C_2H_5N_2NaO_5$ (GSN) has been investigated in order to obtain its band structure. However, thermal stability and mechanical properties for GSN have not been reported in the literature. Besides, we used for the first time, the dielectric properties to evaluate the second derivative of $\varepsilon_2(E)$ and to obtain the number of allowed optical transitions in GSN. In addition, we evaluated the second derivative of ε2

(*E*) function in the density of states. Therefore, a complementary study for GSN crystals not only including thermal, mechanical, and dielectric properties but also containing its relationship between molecular character and properties, all of them are presented in this work.

Methods and computational details

Crystal growth

GSN crystals were grown by the slow cooling technique with a temperature lowering rate of 1 °C/day in the range from 40 to 22 °C starting from saturated aqueous solution which was reported elsewhere [9]. The starting reagents were glycine JT-Baker 98.8% pure and sodium nitrate JT-Baker with a purity of 99.99%.

Thermal analysis

The sample was analyzed in a TA Instruments STD 2960 using simultaneous differential thermal and thermogravimetric analysis (DTA-TGA) mode, and it was heated at the rate of 15 °C/min 50 cm^3 of air, from 25 to 700 °C. In order to confirm the crystalline structure of the synthesized material, powder diffraction patterns for GSN at room temperature and GSN burned at 190°C for an hour were taken in a X-PERT Philips diffractometer with CuKα (λ=1.540598 Å), using a step of 0.05° for time interval of 10 s, and 2θ scanning between 10° and 60°.

Micro-hardness test

Micro-hardness measurements were carried out by using a Micro-hardness tester FM, Future Tech MH-001, fitted with a diamond indenter. GSN crystals were tested on

different faces and the micro-hardness measurements for applied load were made with magnitudes from 10 to 200 g and a time interval of 10 s.

Computational details

The first-principles calculations, involving no adjustable parameters, are based on an explicit quantum treatment of the electrons in a model system, which means solving Schrodinger's equation to find the electronic ground state.

All calculations were performed using Materials Studio 3.2 software [10]. In order to calculate the dielectric properties, module CASTEP (Cambridge Serial Total Energy Package) was employed [11]. CASTEP is a program that employs DFT to simulate the properties of solids, it is based on the pseudopotential plane-wave basis set total energy first-principles method within the framework of DFT for calculation of the Kohn–Sham equations [12,13].

Generalized gradient approximations (GGA) in the scheme of Perdew, Burke, and Erzerhof (PBE) [14] for exchange and correlation effects were employed. Normconserving pseudopotentials were employed to obtain dielectric properties. To confirm the convergence of calculations, they were optimized with respect to the cutoff of energy required in calculations of solid state with the scheme of Lin et al. [15]. Total energy dependence on the energy cut-off (Ecut) was of 770.0 eV that corresponds to a criterion of convergence of 0.1×10^{-5} eV/atom. In both cases optical properties were calculated with 250 k points in the Brillouin zone. GSN exhibits a monoclinic noncentrosymetric crystalline structure with space group Cc. Its lattice parameters are *a*= 14.329 Å (3), b = 5.2662 Å (11), *c* = 9.1129Å (18), and β = 119.10° (3) [16,17].

Results and discussion

The smallest single crystals of GSN (~5mm large) were selected from the solution because they have better geometrical shape than bigger ones and they lack macrodefects. These crystals were employed for micro-hardness test since they have flat surfaces to indenter them. A typical growth habit for these crystals is shown in Fig. 1. It was observed that the smallest GSN crystals have a pyramidal shape with 10 developed faces: {2 0 0}, {0 0 2}, {2 0 2}, and {1 1 0}. The faces {2 0 0}, {0 0 2}, and {2 0 2}, were more elongate along the b crystallographic axis as a result of the alignment of the glycine molecules through the strong hydrogen bonding interaction N–H…O. These hydrogen bridges are common when aminoacids crystallize, because aminoacids have a bipolar structure inside the crystals due to the deprotonation of carboxylic group (COO-) and protonation of amine group (NH_3^+). Furthermore, we can see that glycine molecules formed alternating layers with $NaNO_3$ parallel to the *bc* plane; thus they overlap each other and make (2 0 0) faces which are shown in Fig. 1c.

Thermal analysis

GSN DTA-TGA is shown in Fig. 2. TGA revealed that GSN decomposes in four stages. From the DTA curve, it was found that GSN is stable up to 198°C, because no endothermic signals were observed, which characterize crystalline transformations, and phase changes. In the range from 198 to 226°C an endothermic signal was observed that corresponds to the beginning of a phase change for GSN, until it melted completely, which was followed by two exothermic decomposition signals with temperatures of 302.5 and 396.6°C. They correspond to the combustion of glycine

molecules and to the decomposition of $NaNO_3$, respectively. TGA shows a loss of mass at 226 1C, this is in accordance with the decomposition of the organic part shown in TGA. At elevated temperatures this decomposition process continues up to 700°C. Moreover, it was observed that 2.4% of the water contained in the material was lost before being fused. In order to confirm that GSN keeps its crystal structure we made a powder diffraction experiment for GSN exposed at 190 °C for an interval of 1 h. The pattern is shown in Fig. 3. We clearly see that GSN keeps its crystalline structure at this condition and the SHG process is possible.

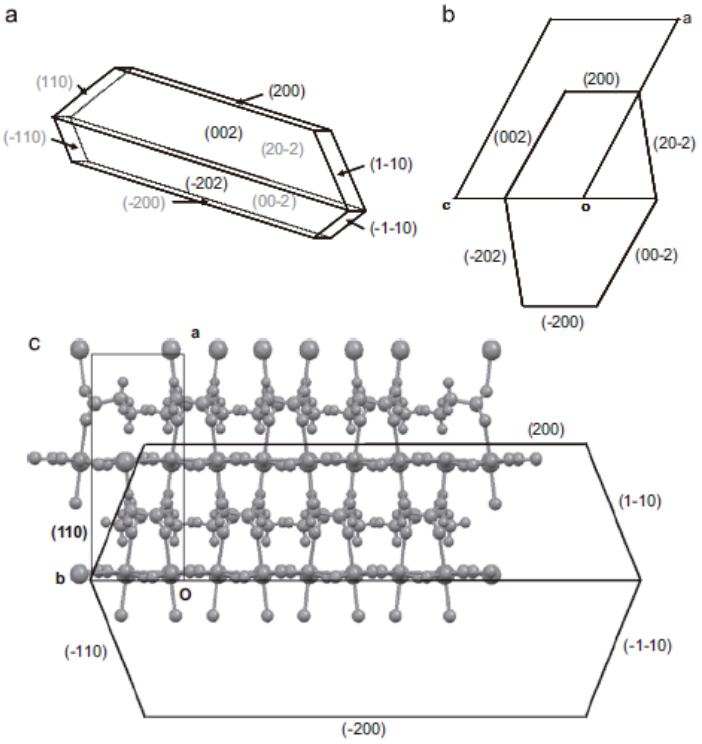

Fig. 1. Growth habit for the GSN crystals analyzed.

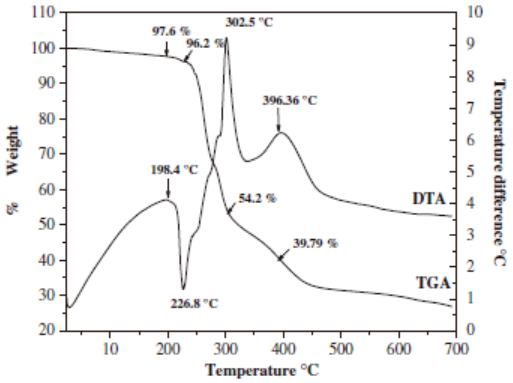

Fig. 2. DTA-TGA curves for GSN.

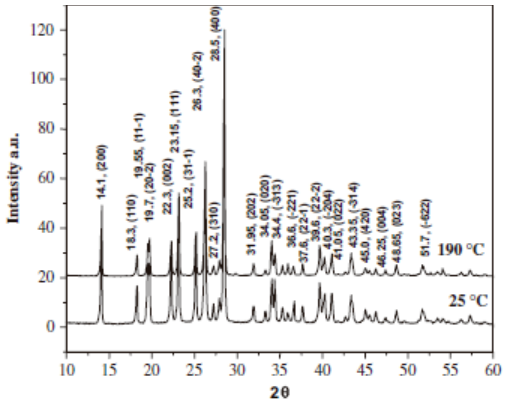

Fig. 3. X-ray powder diffraction patterns of GSN.

Hardness

Hardness of a material is a measure of the resistance that materials present to local deformation and it is an important mechanical property of the optical materials for fabrication of devices. It can be used as a suitable measure for the strength of a material. The Vicker's hardness number was calculated using the relation:

$$H_V = \frac{1.8544(P)}{d^2}$$

where H_V is the Vicker's Hardness number, *P* is the applied load, and *d* is the diagonal average length of the indentation impression. The micro-hardness value was calculated as the average of 30 readings at different faces of GSN ({2 0 0}, {0 0 2}) which belong to five crystals free from visible inclusions and cracks. Arithmetic values of measurements were used for the calculation of hardness. Differences in the values of the five crystals were mainly due to the molecular character and crystal structure of GSN which causes anisotropy.

A plot of the average for the five crystals between the hardness number and the load is depicts in Fig. 4. We clearly can see that the micro-hardness number increases with increasing load. Above 50 g, cracks were developing on the surface of the crystals due to the release of internal stresses generated by indentation. The mechanical properties of GSN are in relation to the long intermolecular distances between layers of glycine and sodium nitrate.

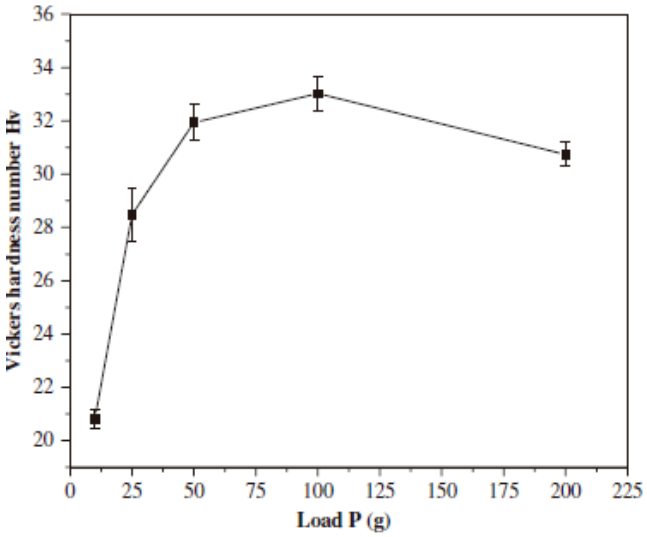

Fig. 4. Average of Vicker's hardness measurements of GSN.

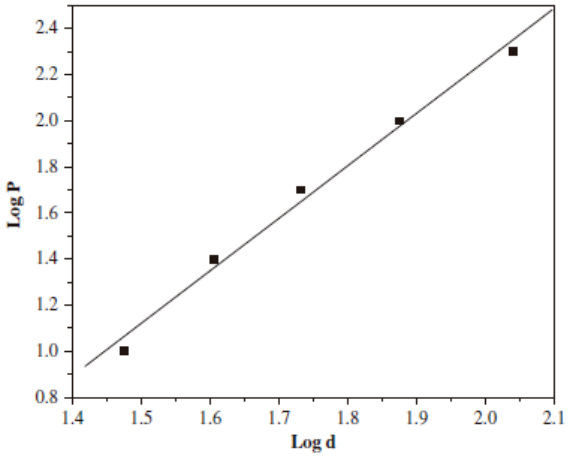

Fig. 5. Meyer's plot of log(P) versus log(d).

The work hardening coefficient (*n*) for a given material in relation to the load (*P*) is given by Meyer's law [18]:

$$P=Ad^n$$

where *A* is an arbitrary constant for a given material, d is an indentation diagonal under an applied test load *P*, and *n* is the Meyer's index or work hardening exponent. The plot log(*P*) versus log(*d*) can be fitted in a straight line (Fig. 5). The value of n was calculated using the least-square fitting method. The coefficient n was found to be 2.27.

If the value of *n* is between 1 and 1.6, the material is moderately hard, if *n* is above 1.6, the material is soft [19, 20]. The n value observed suggested that GSN is a soft material, proving its mechanical strength.

Dielectric properties

The dielectric function is characterized by the dispersive part ε_1 (*E*) and the dissipative part ε_2 (*E*). ε_1 (*E*) part is in some way responsible for the optical absorption in materials. In the case of GSN we obtained the dielectric function with GGA calculations with light polarized parallel to Y dielectric axis.

Fig. 6, shows the values for the dielectric constant obtained with GGA of GSN. The low value of ε_1 (*E*) between 0.0 and 3.0 eV is an important characteristic of GSN. Besides, the linear behavior of ε_2 (*E*) from 0.0 to 3.0 eV agrees with the optical transparency of GSN. These features promised that GSN has good optical properties. Besides, the calculated density of states is shown in Fig. 7. DOS was produced with a smearing with of 0.2 eV, with the Fermi level placed at 0 eV.

Measurements of absorption spectra of solids present a number of difficulties. These arise principally as a result of the high concentration of matter which leads to very strong optical absorbance. Consequently, the absorbance bands for GSN were overlapped and look like single bands.

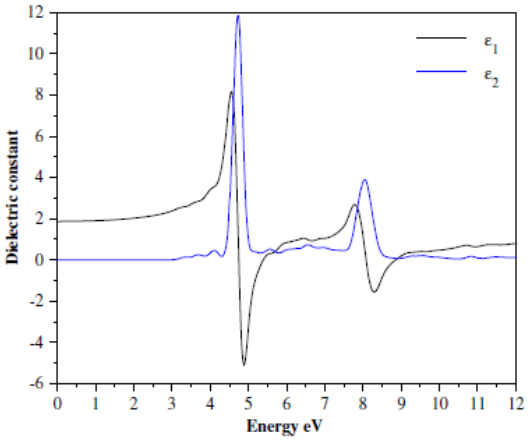

Fig. 6. Dielectric constant of GSN.

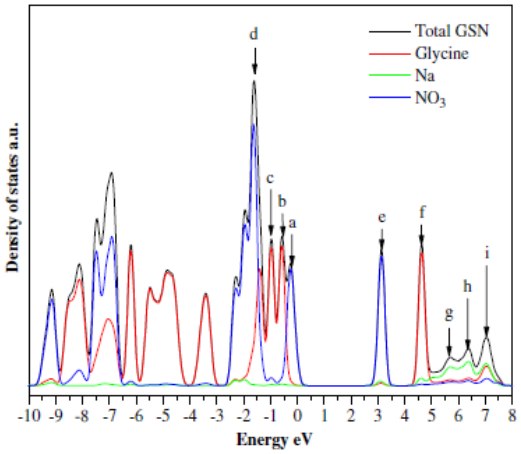

Fig. 7. Total density of states (DOS) of GSN.

For this reason we analyzed the imaginary part of the dielectric constant in order to obtain information about the electronic transitions, which form the absorption bands in GSN.

The second derivative of $\varepsilon_2(E)$ provides a measurement of the numbers of possible optical transitions between electronic states of the valence band and the conduction band. Thus, the use of second derivative of $\varepsilon_2(E)$ is a common artifact when the exact position in energy of maximum is required. In summary, the position on energy of the main peaks gives the allowed electronic transition in a material.

The plot of second derivative of $\varepsilon_2(E)$ versus the energy parallel to the Y dielectric axis in GSN crystal is shown in Fig. 8. The maximum values correspond to the allowed electronic transitions. As it was expected, the maximum values of second derivative of $\varepsilon_2(E)$ matched with the DOS representation for GSN (Fig. 7). These results are present in Table 1.

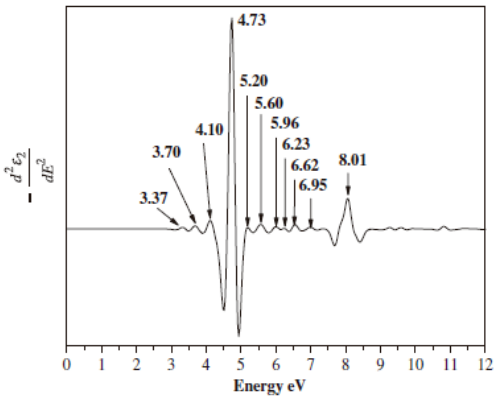

Fig. 8. Second derivative of $\varepsilon_2(E)$ obtained for GSN along Y dielectric axis.

Table 1
Electronic transition for GSN along Y direction

Transition	Δ Energy (eV)
a→e	3.37
b→e	3.70
c→e	4.10
d→e	4.73
b→f	5.20
c→f	5.60
a→g	5.96
d→f	6.23
a→h	6.62
b→h	6.95
c→i	8.01

The second derivative of ε_2 (*E*) suggested that the first optical absorption band can be splitting in three. The first allowed transition at 3.37 eV, was consistent with the band gap parallel at the direction of Y dielectric axis and is due to *a* → *e* transition shown in Fig. 7 and it belongs to O2p for NO_3 states, this is showed more clearly in Fig. 9. Additionally, the two following allowed electronic transitions at 3.70 and 4.10 eV are from *b* → *e* and *c* → *e* transitions shown in Fig. 7 and these were due to a combination of the transitions from O2p glycine states to O2p nitrate states (Fig. 9). The second absorption band can be split into seven allowed transitions corresponding to: d → e, b → f, c → f, a → g, d → f and a → h transitions shown in DOS representation. At 8.01 eV other absorption band appears, corresponding to c → I transition (Fig. 7). Moreover, a representation of the energy level diagram for the molecular orbitals was obtained and it is showed in Fig. 10. Clearly we can see that, HOMO and LUMO orbitals belong to NO_3 group, and they are its bonding and antibonding combinations, respectively. On the other hand, HOMO-1 and HOMO-2 are located over both glycine and NO_3 groups. Although, HOMO-3 resided mainly over NO_3 group and it has a small contribution of glycine. LUMO +1 orbital is located over glycine molecule. Finally LUMO +2 orbital belongs mainly to Na atom.

By analyzing these results, we can see that the electronic transitions in GSN have a molecular character, due to the electronic transitions involved glycine and sodium nitrate orbitals.

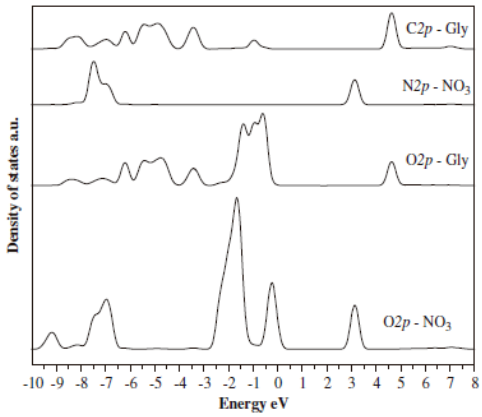

Fig. 9. DOS for 2p orbitals of GSN.

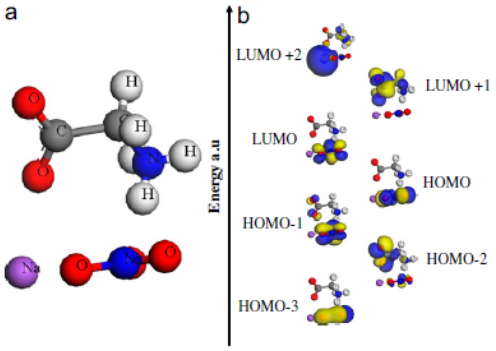

Fig. 10. (a) Single molecule of GSN. (b) The shape of orbitals for GSN.

Conclusion

Thermal analysis showed that GSN is stable up to 198°C. Besides, GSN kept its crystalline structure after it was heated at 190° C for 1 h and it can allow SHG process. Maximum value of H_V = 33 Kg/mm2 was found. Variation of the Vicker's microhardness follows the pattern hardness increases with the increase of load. Micro-hardness of GSN crystals was influenced by the molecular arrangement inside the crystals. In addition, anisotropy in different faces at different planes was found. The dielectric response of GSN has been associated with its electronic structure. We confirmed that, by evaluating the second derivative of $\varepsilon_2(E)$, it is possible to separate the wide bands observed in the absorption spectra and to obtain better resolution of the electronic

transitions involving the energy bands. In the case of GSN, these transitions were matched accurately with the DOS representation and they gave information of the absorbent groups. This information is valuable for designing novel molecular materials for NLO applications by computational chemistry. DFT was confirmed to be an important tool for the calculation and optimization of properties of the new materials.

Acknowledgements

Authors acknowledge Roal Torres and Daniel Lardizaval (Centro de Investigación en Materiales Avanzados S.C.) for their technical support and Marco Gallo for his valuable comments about computational methods. J. Hernández-Paredes gratefully acknowledge a doctoral fellowship provided by CONACYT (National Council of Science and Technology in México).

References

[1] H.A. Petrosyan, H.A. Karapetyan, M.Yu. Antipin, A.M. Petrosyan, J. Cryst. Growth 275 (2005) e1919–e1925.

[2] C. Razzetti, M. Ardoino, L. Zanotti, M. Zha, C. Paorici, Cryst. Res. Technol. 37 (2002) 456–465.

[3] S. Haussuhl, H.A. Karapetyan, R.P. Sukiasyan, A.M. Petrosyan, Cryst. Growth Des. 6 (2006) 2041–2046.

[4] Ra. Shanmugavadivu, G. Ravi, A. Nixon Azariah, J. Phys. Chem. Sol. 67 (2006) 1858–1861.

[5] M.D. Aggarwal, J. Stephens, A.K. Batra, R.B. Lal, J. Optoelectron. Advan. Mater. 5 (2003) 555–562.

[6] Bohdan Andriyevsky, Wioleta Ciepluch-Trojanek, Mykola Romanyuk, Aleksy Patryn, Marcin Jaskolski, Physica B 364 (2005) 78–84.

[7] B. Andriyevsky, V. Kapustianyk, W. Ciepluch-Trojanek, A. Batiuk, Physica B 367 (2006) 216–222.

[8] B. Andriyevsky, N. Esser, A. Patryn, C. Cobet, W. Ciepluch-Trojanek, M. Romanyuk, Physica B 373 (2006) 328–333.

[9] J. Herna´ndez-Paredes, D. Glossman-Mitnik, H.E. Esparza-Ponce, M.E. Alvarez-Ramos, A. Duarte-Moller, J. Mol. Struct. 875 (2008) 295.

[10] Materials Studio version 3.2, Accelrys Inc. San Diego, 2001.

[11] V. Milman, B. Winkler, J.A. White, C.J. Pickard, M.C. Payne, E.V. Akhmatskaya, R.H. Nobes, Int. J. Quant. Chem. 77 (2000) 895–910.

[12] P. Hohenberg, W. Kohn, Phys. Rev. 136 (1964) B864–B871.

[13] W. Kohn, L.J. Sham, Phys. Rev. 140 (1965) A1133–A1138.

[14] J.P. Perdew, K. Burke, W. Ernzerhof, Phys. Rev. Lett. 77 (1996) 3865–3868.

[15] J.S. Lin, A. Qteish, M.C. Payne, V. Heine, Phys. Rev. B 47 (1993) 4174–4180.

[16] R.V. Krishnakumar, M. Subha Nandhini, S. Natarajan, K. Sivakumar, Babu Varghese, Acta. Cryst. C 57 (2001) 1149–1150.

[17] M. Narayan Bhat, S.M. Dharmaprakash, J. Cryst. Growth 235 (2002) 511–516.

[18] M.A. Meyer, Some aspects of the hardness of metals, Ph.D. Thesis, Dreft (1951).

[19] E.M. Onitsch, Mikroskopie 2 (1947) 131–194.

[20] M. Hanneman, Metall. Manchu 23 (1941) 135.